JOURNAL OF BACTERIOLOGY, Mar. 1990, p. 1180–1185
0021-9193/90/031180-06$02.00/0

Vol. 172, No. 3

Microbial Growth Patterns Described by Fractal Geometry

MARTIN OBERT,[1]* PETER PFEIFER,[2] AND MANFRED SERNETZ[1]

Institut für Biochemie und Endokrinologie, Justus-Liebig-Universität Giessen, Frankfurterstrasse 100, D-6300 Giessen, Federal Republic of Germany,[1] and Department of Physics, University of Missouri-Columbia, Columbia, Missouri 65211[2]

Received 3 July 1989/Accepted 20 November 1989

Fractal geometry has made important contributions to understanding the growth of inorganic systems in such processes as aggregation, cluster formation, and dendritic growth. In biology, fractal geometry was previously applied to describe, for instance, the branching system in the lung airways and the backbone structure of proteins as well as their surface irregularity. This investigation applies the fractal concept to the growth patterns of two microbial species, *Streptomyces griseus* and *Ashbya gossypii*. It is a first example showing fractal aggregates in biological systems, with a cell as the smallest aggregating unit and the colony as an aggregate. We find that the global structure of sufficiently branched mycelia can be described by a fractal dimension, D, which increases during growth up to 1.5. D is therefore a new growth parameter. Two different box-counting methods (one applied to the whole mass of the mycelium and the other applied to the surface of the system) enable us to evaluate fractal dimensions for the aggregates in this analysis in the region of $D = 1.3$ to 2. Comparison of both box-counting methods shows that the mycelial structure changes during growth from a mass fractal to a surface fractal.

Fractal analysis (8, 13, 15) introduced to microbiology to describe growth patterns is of fundamental importance: morphological differences of mycelial structures correlate with pathogenicity (7) as well as with growth, metabolic activity, enzyme production (6), and pigmentation (11). At present, mycelia are described as diffuse, compact, smooth, rough, etc. (1, 4, 9–11, 17, 18). Because of the complex structure of mycelia, a geometric, pattern-oriented description, which leads to a measure of irregularity, was impossible without the development of fractal geometry. Other applications of fractal geometry to biological systems are described elsewhere (2, 3, 5, 12, 14, 16).

MATERIALS AND METHODS

Strains, materials, and methods. Method 1. *Streptomyces griseus* (DSM 40693) was grown under the following conditions. A cover slip was deposited on a filter paper in a petri dish. After dry sterilization, the filter paper was wetted with 2 ml of sterile water. Next, the cover slip was coated under sterile conditions with 20 μl of a 3-day-old spore suspension containing 2.5% standard nutrient solution (Merck 7882, diagnostic). Incubation temperature was 28°C.

Method 2. *Ashbya gossypii* (ATCC 10895) was grown as follows. A cover slip was coated with a layer of agar (Merck no. 1615, DAB 6), 0.5 mm thickness, containing 2.5% standard nutrient solution (Merck no. 7882, diagnostic). The cover slip was then deposited on a glass slide on a wet filter paper in a petri dish. After wet sterilization, the petri dish was cooled in a perfectly horizontal position (monitored by a bubble level). The cover slip was then inoculated with 20 μl of spore suspension under sterile conditions so as not to damage the agar layer. Incubation temperature at 28°C.

Light microscopy and image processing. All methods have to ensure that the mycelial structure is not damaged by any applied technique. Therefore, no cover slip is used to cover a mycelium for microscopy. In method 1, a photograph of the mycelium of *S. griseus* is taken with a phase-contrast microscope (Leitz Diavert) and a camera. The hard copy of the photograph is digitized by a high-resolution camera (Aqua-tv) connected to a personal computer (Sperry-AT) with 512 × 512 pixel resolution, PIP-512/1024 graphic card (Matrox Electronic Systems), and a standard image analysis system (Soft-Imaging System, Münster, Federal Republic of Germany).

Method 2 is applied to young mycelia of *A. gossypii* in which the whole mycelium can be magnified by the microscope in one image. Photographs of the mycelia are taken by a dark-field microscope (Leitz Laborlux) connected to a high-resolution camera and a video recorder. The same equipment is used as in method 1, even if such is not specifically mentioned. The data of the images are transferred from the video recorder to the computer by the image analysis system.

Method 3 is applied in those cases where only a part of the mycelium can be magnified by the microscope in one image. The data of the images of all parts of a mycelium are stored on a videotape (dark-field microscopy; high-resolution camera connected to a video recorder). The video recorder is then connected to a television, and photographs are taken from the screen. After that, the structure of the mycelium is reconstructed by a puzzle technique from the individual photographs. To enhance contrast, the background of the hyphal structure is drawn in black. The resulting image, which shows the whole mycelium, is digitized as described in method 1.

Box-counting methods and fractal terminology. Methods and terminology have been described previously (15). Evaluation of the fractal dimension D in terms of the box-counting method can be carried out as follows. Cover the mycelium with a grid of cells (boxes) of side length ε and count how many boxes, $N_{box}(\varepsilon)$, are intersected by the mycelium. The number of boxes $N_{box}(\varepsilon)$ grows as ε^{-D}. Thus, if a mycelium has a well-defined fractal dimension D, we should find that

$$N_{box}(\varepsilon) = C\varepsilon^{-D} \quad (1)$$

C is a proportionality constant. Power law 1 can be fulfilled

* Corresponding author.

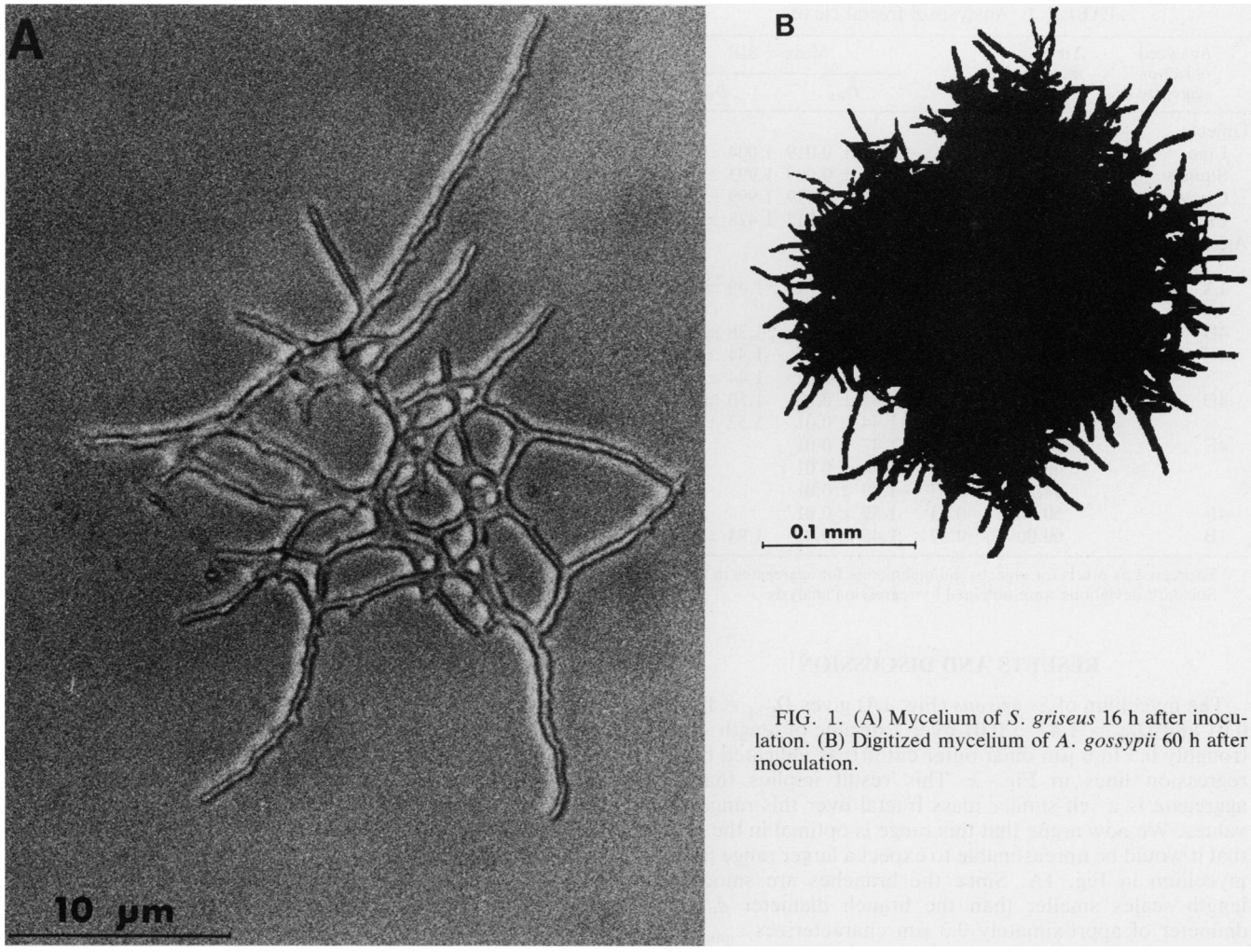

FIG. 1. (A) Mycelium of *S. griseus* 16 h after inoculation. (B) Digitized mycelium of *A. gossypii* 60 h after inoculation.

only within the following ε range: the diameter of a hypha d_0 sets a natural lower limit (inner cutoff, ε_{min}), and the diameter L of the aggregate sets an upper limit (outer cutoff, ε_{max}).

Mycelial structures can be mass fractals (the whole mass of the organism is fractal) or surface fractals (only the surface [border] is fractal) (15). To distinguish between these two kinds of fractals, we apply two different box-counting methods. The box mass (BM) method is applied to the whole mass of the mycelium, which leads to the box mass dimension, D_{BM}. In the box surface (BS) method, only those boxes that cover the surface (border) of the mycelium have to be counted. The BS method leads to the box surface dimension, D_{BS}. These box-counting evaluations of the digitized mycelial structures are performed by computer.

In the case of a mass fractal, the two methods give the same values of D_{BM} and D_{BS}. Here the fractal dimension D is equal to D_{BM}, which is equal to D_{BS}. For a surface fractal, we can no longer describe the object by one single dimension D. The D_{BS} value describes the surface irregularities and is equal to the fractal dimension D. The D_{BM} value describes the dimension of the embedding space d. In this analysis, the d value is equal to 2, based on the analysis of photographs, which are planar projections of objects that grow in $d = 2$ or 3.

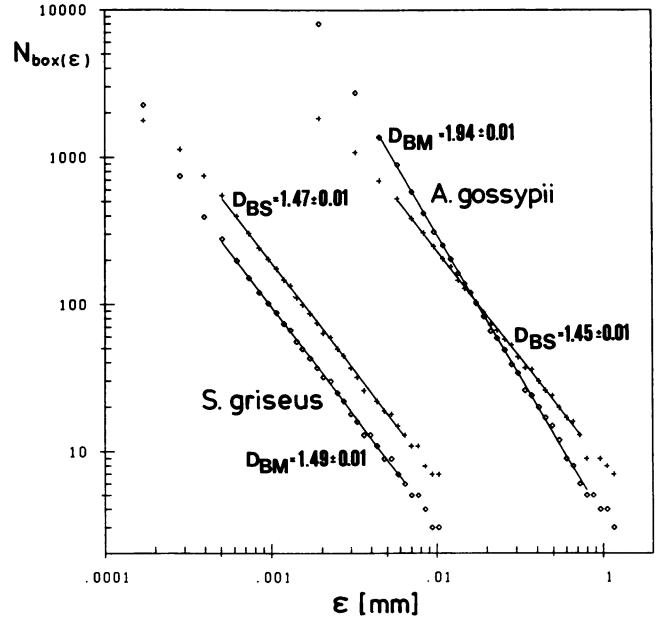

FIG. 2. Evaluation of the mycelia shown in Fig. 1. Experimental values of number of boxes $N_{box}(\varepsilon)$ versus box length ε(mm), determined by the BS (+) and BM (◇) methods. Scaling behavior was well over 1 decade, as indicated by the regression lines.

TABLE 1. Analysis of fractal curves

Analyzed object or aggregate	Time after inoculation (h.min)	L^a	Mean ± SD[b]	
			D_{BS}	D_{BM}
Object				
Line		512	1.004 ± 0.019	1.004 ± 0.019
Square		424	1.002 ± 0.009	1.993 ± 0.027
Circle		349	1.000 ± 0.019	1.999 ± 0.011
Fig. 3		512	1.428 ± 0.012	1.428 ± 0.012
Aggregate in given figure				
1A	16.00	0.038	1.47 ± 0.01	1.49 ± 0.01
4A	17.45	0.10		
4B	21.50	0.25	1.34 ± 0.01	1.36 ± 0.02
4C	25.00	0.33	1.42 ± 0.01	1.44 ± 0.01
	27.10	0.39	1.40 ± 0.01	1.44 ± 0.01
4D	30.50	0.50	1.44 ± 0.01	1.50 ± 0.01
	34.10	0.51	1.44 ± 0.01	1.52 ± 0.01
4E	36.50	0.51	1.47 ± 0.01	
	40.40	0.52	1.46 ± 0.01	
	44.55	0.53	1.49 ± 0.01	
4F	50.30	0.53	1.52 ± 0.01	
1B	60.00	0.37	1.45 ± 0.01	1.94 ± 0.01

[a] Expressed as pixels for objects and millimeters for aggregates in figures.
[b] Standard deviations were obtained by regression analysis.

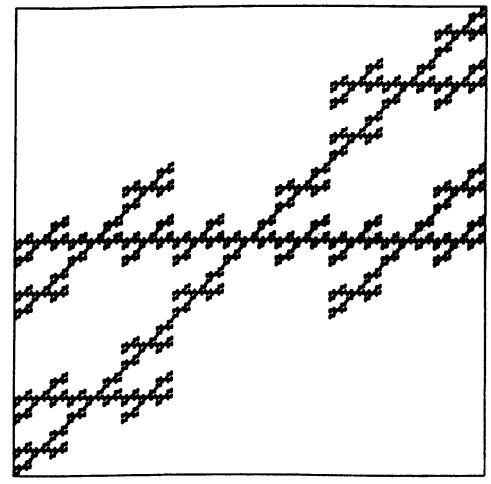

FIG. 3. Algorithmically constructed self-similar curve. Self-similarity means that the system can be decomposed into parts geometrically similar to the whole object. See reference 15 for a detailed description of how to generate such fractal curves. Here the fractal dimension can be calculated analytically: $D = \log 5/\log 3 \approx 1.4649$. The experimental analyses by the BM and BS methods yield a value of 1.428 for D_{BM} and D_{BS}, with a standard deviation of 0.012. However, the difference of $D-D_{BM}$ or $D-D_{BS}$ equals 0.037 for this mass fractal.

RESULTS AND DISCUSSION

The mycelium of *S. griseus* (Fig. 1A) gives $D_{BM} = 1.49 \pm 0.01$ and $D_{BS} = 1.47 \pm 0.01$ over 1 decade of length scales (roughly 0.5 to 6 μm inner/outer cutoff), as indicated by the regression lines in Fig. 2. This result implies that the aggregate is a self-similar mass fractal over this range of ε values. We now argue that this range is optimal in the sense that it would be unreasonable to expect a larger range for the mycelium in Fig. 1A. Since the branches are smooth at length scales smaller than the branch diameter d_0, this diameter of approximately 0.3 μm characterizes ε_{min}. The diameter L of the mycelium is approximately 38 μm. The analysis of deterministic fractal curves by the BM and BS methods shows that ε_{max} is found in the range $L/3.5$ to $L/4.5$ (2). Thus, the inner and outer cutoffs found from Fig. 2 are indeed optimal.

The quality of the standard deviations of the D_{BM} and D_{BS} values from the regression analysis should not be overestimated if the box-counting methods are performed with a 512 × 512 pixel resolution image analysis system. To detect the range of real error, we analyze deterministically constructed fractal curves (Fig. 3), for which it is possible to calculate D analytically as well as experimentally by the BM or BS method. With such fractal curves (Fig. 3 and Table 1) as test objects for the BM and BS methods, we find deviations in the following range: $-0.01 < D-D_{BM} < 0.04$ and $0 < D-D_{BS} < 0.04$. This range is valid only if the standard deviation of D_{BM} or D_{BS} obtained by regression analysis is less than or close to 0.02. This is in agreement with results found by Farin et al. (2).

The mycelium shown in Fig. 1A grows in $d = 2$, whereas the mycelium of *A. gossypii* in Fig. 1B grows embedded in the three-dimensional space. The evaluation of this aggregate gives $D_{BS} = 1.45 \pm 0.01$ and $D_{BM} = 1.94 \pm 0.01$. This D_{BM} value is close to the value of 2 that we would expect for a planar photographic projection for such a surface fractal. In this aggregate, hyphae grow above each other and fill the area completely in the center. Hyphae also grow into the agar layer as well as into the air. Information about a pore

TABLE 2. Values of various cutoffs and expected cutoffs to show the major domain affected by the filled center part on the double logarithmic plot[a]

Determination for given figure	Value (mm)							
	Log ε_{min} expected	Log ε_{min}	Log $(d_0'/4)$	Log ε_{max} expected	Log ε_{max}	Log L	Log ε_{min} − log $(d_0'/4)$	Log $(d_0'/4)$ − log ε_{max}
Cutoff and expected cutoff								
4E	−2.43	−2.38	−1.94	−0.86	−0.89	−0.29		
4F	−2.43	−2.36	−1.57	−0.97	−0.89	−0.29		
1B	−2.43	−2.43	−1.30	−1.09	−1.03	−0.43		
Range of scaling behavior								
4E							−0.44	−1.08
4F							−0.79	−0.60
1B							−1.13	−0.21

[a] The larger the region of scaling behavior log ε_{min} − log $(d_0'/4)$, the larger the influence of the filled center part. The differences between ε_{min} and ε_{min} expected (which is d_0) as well as between ε_{max} and ε_{max} expected (which is $L/4$) are small in all cases.

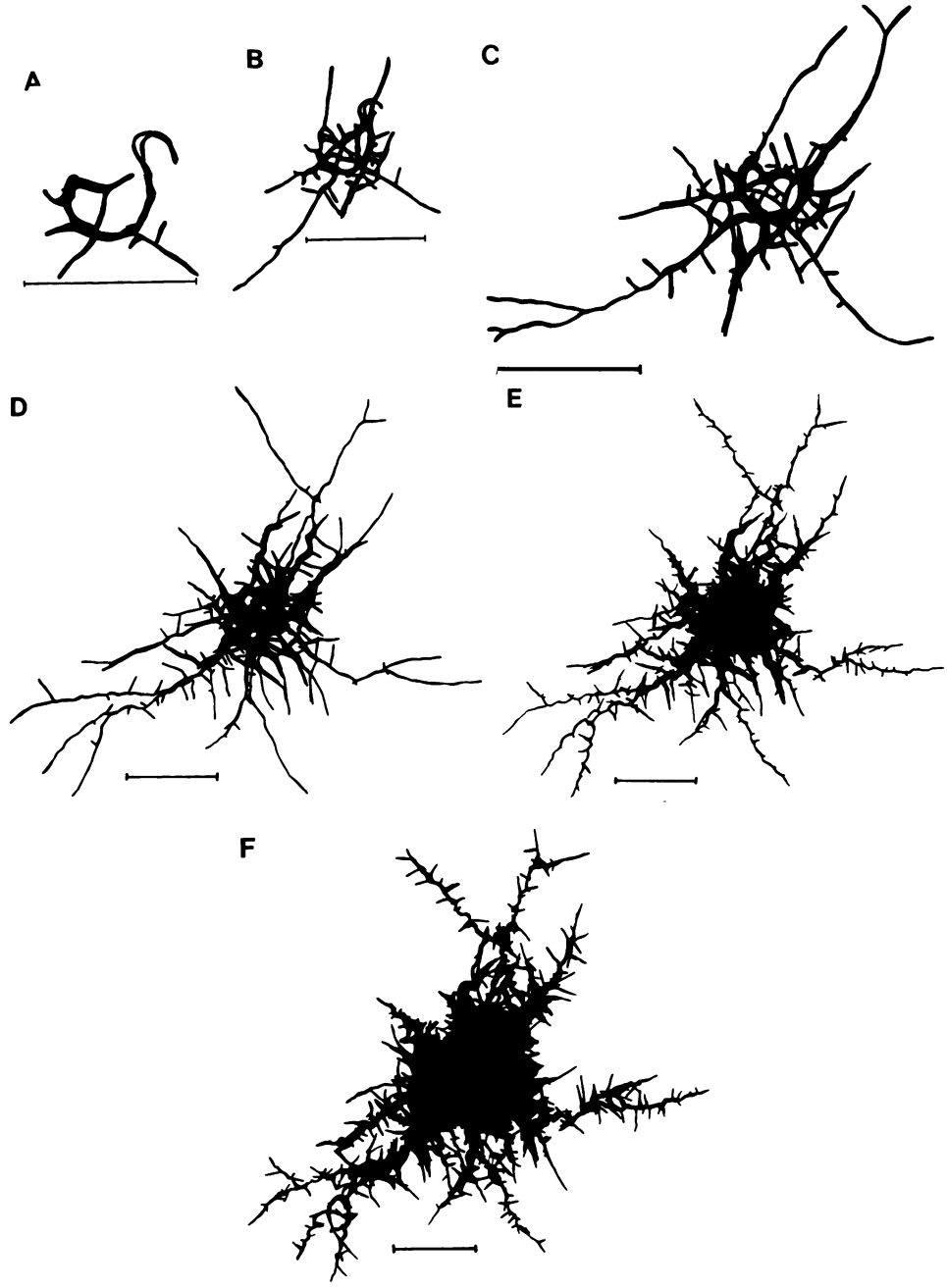

FIG. 4. Development of a mycelial structure of *A. gossypii* after consecutive time steps. Bars = 0.1 mm.

structure is lost in the projection. Clearly, other methods are required to study such out-of-plane growth.

A spore of *A. gossypii* grows into a straight or a zigzag hypha which, under fractal analysis, should yield a D value close to 1. Later branching occurs as shown in Fig. 4A. For this mycelium, we do not find a well-defined power law in Fig. 5, and we cannot draw a regression line in this case. This is reasonable because the fractal behavior here is naturally associated with the branching of hyphae. In such a young mycelium, we do not find a sufficient number of branches to allow for a power law of type given in equation 1. Consecutive photographs show vegetative mycelia with $D_{BM} = D_{BS}$ (mass fractal) in the region from 1.35 to 1.45. Here the hyphae grow on the agar layer embedded in $d = 2$ (we disregard the few hyphae that grow into the agar layer). In later stages of colony growth (here approximately from Fig. 4D), the diameter of the mycelium increases very slowly (Fig. 4 and Table 1). Instead, we find more and more space-filling growth. At this stage of growth, we find a transition from a mass fractal to a surface fractal. D_{BS} converges to a value of approximately 1.5 (Fig. 6).

We now want to know how to explain the D_{BM} value if the filled center part of an object is not sufficiently large in surface fractals. The analysis of the surface fractals in Fig. 4 by the BM method shows a slow increase of "D_{BM}," although a value of 2 might be expected. To explain this behavior, we correlate the diameter of the largest circle that covers the two-dimensional filled center of the mycelium, d_0', and the mycelium diameter L. We find the following. In Fig. 4B and C, $D_{BS} = D_{BM}$ and $d_0'/L < 0.05$, which is

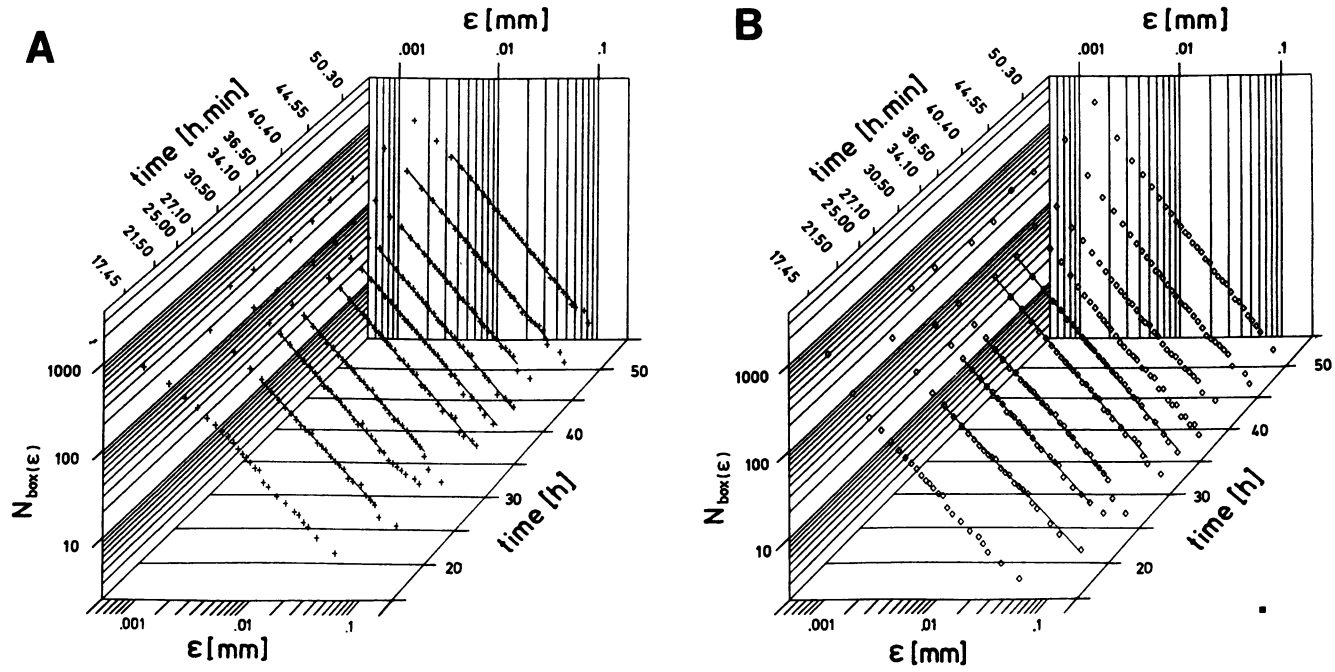

FIG. 5. Experimental values of the mycelium shown in Fig. 4: number of boxes $N_{box}(\varepsilon)$ versus box length ε(mm) versus time. The exact times of the consecutive photographs are shown at the top of the left margin. A well-defined power law behavior (equation 1) is indicated by a drawn regression line. Scaling behavior is in the range of 1.0 to 1.4 decades. (A) Data analyzed by the BS method. (B) Data analyzed by the BM method.

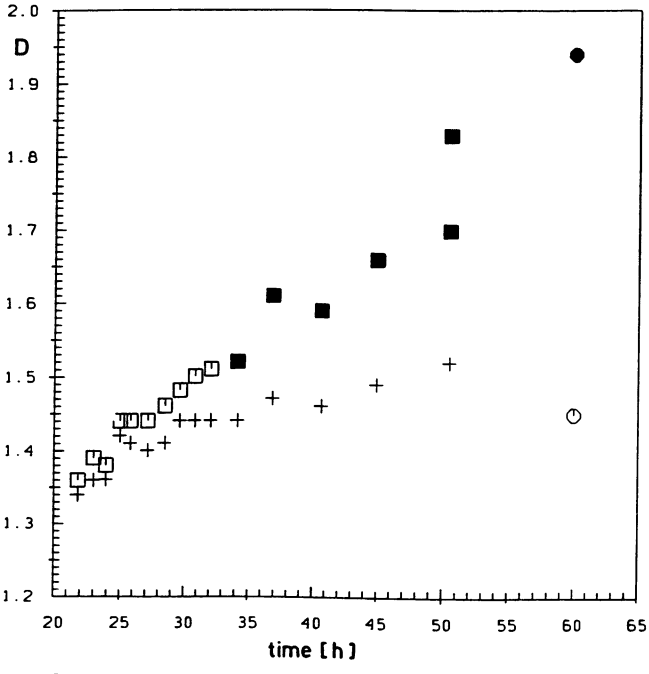

FIG. 6. Function of the fractal dimension D_{BS} (+) and D_{BM} (□) versus time of the mycelial development of *A. gossypii* from Fig. 4. ■, Values of "D_{BM}" for which the BM method does not lead to a well-defined power law behavior (equation 1) because of the d_0' problem. These "D_{BM}" values may not be interpreted as a fractal dimension. ○, D_{BS} value of the mycelium shown in Fig. 1B. The D_{BM} value of this aggregate (●) is close to $d = 2$. The standard deviations from the regression analysis of D_{BS} or D_{BM} are below 0.02. All correlation coefficients are better than −0.998.

negligible for the d_0' problem. In the range of $0.05 < d_0'/L < 0.1$ (Fig. 4D), D_{BM} is close to D_{BS}. For Fig. 4E and F, we find that $d_0'/L > 0.1$. Here there is a significant divergence between D_{BS} and "D_{BM}."

In the consecutive time steps of the mycelial development, the quotient d_0'/L increases slowly. Therefore, it is reasonable to expect a slightly increasing divergence of the D_{BM} and D_{BS} values in the function $D_{BM}(\text{time}) - D_{BS}(\text{time})$ rather than a strong transition.

Furthermore, we now ask where the major influence of the filled center part in the double-logarithmic plot can be found. We have shown that the scaling behavior ends with a box size ε of approximately $L/4$. We therefore argue that it should be possible to find the influence of the filled center part on the double-logarithmic plot at a box size ε of roughly $d_0'/4$. For Fig. 4E, we find that $d_0'/4$ is too close to the inner cutoff to allow for a strong divergence between D_{BS} and D_{BM}. The detailed values are shown in Table 2. In case of Fig. 4F, $d_0'/4$ lies between the inner cutoff and outer cutoff. Here we cannot find a well-defined D_{BM} value in the expected range d_0 to $L/4$. Instead, we find a value of 1.70 ± 0.01 in the range $L/4$ to $d_0'/4$ and a second value of 1.83 ± 0.02 in the range of $d_0'/4$ to d_0. In the case of Fig. 1B, we find that $d_0'/4$ is sufficiently close to $L/4$ to allow for an approximation of the embedding dimension $d = 2$ by the D_{BM} value of 1.94 ± 0.01 in the range of $d_0'/4 \approx L/4$ to d_0.

We have shown that fractal geometry is suitable to describe biological growth patterns for two particular strains (a bacterium and a fungus) and different sets of growth conditions (with and without agar). We have shown that the fractal dimension increases during growth. Therefore, it seems likely that for a wide variety of microorganisms and under a wide variety of growth conditions, the fractal dimension as explored here may serve as an important morphological characteristic of mycelial growth. We have shown that

sufficiently branched mycelia are self-similar. This property implies that the global structure of an object may be complex, although the fundamental growth concept—the way to generate the complex system—may be very simple (13).

An important task will thus be to study the dependence of D on different strains in the presence of chemical compounds affecting growth. This could mean a new microbiological test. Another practical application might be to correlate D with antibiotic concentrations in order to optimize fermentation processes; the shape of an organism may have a significant effect in a fermentation process. On the other hand, one may wish to develop theoretical models to explain the observed fractal behavior. These models would have to ensure that D increases during growth and that the aggregate performs the transition from a mass to a surface fractal. Clearly, such models will have to be very different from the aggregation models studied extensively for the formation of inorganic fractal clusters (8).

ACKNOWLEDGMENTS

We thank W. Crueger and P. Wlczek for helpful discussions and U. Neuschulz for laboratory assistance.

We thank the Deutsche Forschungsgemeinschaft (grant Se 315/13-1) for financial support.

LITERATURE CITED

1. **Belisle, J. T., and P. J. Brennan.** 1989. Chemical basis of rough and smooth variation in mycobacteria. J. Bacteriol. **171**:3465–3470.
2. **Farin, D., S. Peleg, D. Yavin, and D. Avnir.** 1985. Applications and limitations of boundary-line fractal analysis of irregular surfaces. Proteins, aggregates, porous materials. Langmuir **1**: 399–407.
3. **Feder, J., T. Jossang, and E. Rosenqvist.** 1984. Scaling behavior and cluster fractal dimension determined by light scattering from aggregating proteins. Phys. Rev. Lett. **53**:1403–1406.
4. **Gull, K.** 1975. Mycelial branch patterns of thamnidium elegans. Trans. Br. Mycol. Soc. **64**:321–363.
5. **Helman, J. S., A. Coniglio, and C. Tsallis.** 1984. Fractons and the fractal structure of proteins. Phys. Rev. Lett. **53**:1195–1197.
6. **Hermersdörfer, H., A. Leuchtenberger, C. Wardsack, and H. Ruttloff.** 1987. Influence of culture conditions on mycelial structure and polygalacturonase synthesis of Aspergillus niger. J. Basic Microbiol. **27**:309–315.
7. **Hubbard, M. J., D. Markie, and R. T. M. Poulter.** 1986. Isolation and morphological characterization of a mycelial mutant of *Candida albicans*. J. Bacteriol. **165**:61–65.
8. **Jullien, R., and R. Botet.** 1987. Aggregation and fractal aggregates. World Scientific, Singapore.
9. **Kretschmer, S.** 1978. Kinetics of vegetative growth of Thermoactinomyces vulgaris. Z. Allg. Mikrobiol. **18**:701–711.
10. **Kretschmer, S.** 1982. Dependence of the mycelial growth pattern on the individually regulated cell cycle in Streptomyces granaticolor. Z. Allg. Mikrobiol. **22**:335–347.
11. **Leblond, P., P. Demuyter, L. Moutier, M. Laakel, B. Decaris, and J.-M. Simonet.** 1989. Hypervariability, a new phenomenon of genetic instability, related to DNA amplification in *Streptomyces ambofaciens*. J. Bacteriol. **171**:419–423.
12. **Lewis, M., and D. C. Rees.** 1985. Fractal surfaces of proteins. Science **230**:1163–1165.
13. **Mandelbrot, B. B.** 1982. The fractal geometry of nature. Freeman, Oxford.
14. **Morse, D. R., J. H. Lawton, M. M. Dodson, and M. H. Williamson.** 1985. Fractal dimension of vegetation and the distribution of arthropod body lengths. Nature (London) **314**: 731–733.
15. **Pfeifer, P., and M. Obert.** 1989. Fractals: basic concepts and terminology, p. 11–43. *In* D. Avnir (ed.), The fractal approach to heterogeneous chemistry. John Wiley & Sons, Inc., Chichester, United Kingdom.
16. **Pfeifer, P., U. Welz, and H. Wippermann.** 1985. Fractal surface dimension of proteins: lysozyme. Chem. Phys. Lett. **113**:535–540.
17. **Schuhmann, E., and F. Bergter.** 1976. Mikroskopische Untersuchungen zur Wachstumskinetik von Streptomyces hygroscopicus. Z. Allg. Mikrobiol. **16**:201–215.
18. **Waterbury, J. B., and R. Y. Stanier.** 1978. Patterns of growth and development in pleurocapsalean cyanobacteria. Microbiol. Rev. **42**:2–44.